ISSN 1674-1056
http://cpb.iphy.ac.cn
http://iopscience.iop.org/cpb
中国物理 B
Chinese Physics
中国物理 Chinese Physics B

Using the $Hg_xMg_{(1-x)}Te$ ternary compound as a room temperature photodetector:Study of the electronic structure, charge transport, and response function of the energetic electromagnetic radiation

Ghasemi Hasan, Mokhtari Ali
Citation: Chin. Phys. B . 2018, 27(5): 053101. **doi:** 10.1088/1674-1056/27/5/053101

Journal homepage: http://cpb.iphy.ac.cn; http://iopscience.iop.org/cpb

What follows is a list of articles you may be interested in

Ab-initio calculations of structural, electronic, and optical properties of $Zn_3(VO_4)_2$

Nisar Ahmed, S Mukhtar, Wei Gao, Syed Zafar Ilyas
Chin. Phys. B . 2018, 27(3): 033101. **doi:** 10.1088/1674-1056/27/3/033101

Improvement of the thermoelectric efficiency of pyrene-based molecular junction with doping engineering

Mohammad Farid Jamali, Meysam Bagheri Tagani, Hamid Rahimpour Soleimani
Chin. Phys. B . 2017, 26(12): 123101. **doi:** 10.1088/1674-1056/26/12/123101

Effects of temperature and pressure on thermodynamic properties of $Cd_{0.25}Zn_{0.75}$ alloy

Najm Ul Aarifeen, A Afaq
Chin. Phys. B . 2017, 26(12): 123103. **doi:** 10.1088/1674-1056/26/12/123103

Correlation between electronic structure and energy band in Eu-doped $CuInTe_2$ semiconductor compound with chalcopyrite structure

Tai Wang(王泰), Yong-Quan Guo(郭永权), Shuai Li(李帅)
Chin. Phys. B . 2017, 26(10): 103101. **doi:** 10.1088/1674-1056/26/10/103101

Tuning the energy gap of bilayer *α* -graphyne by applying strain and electric field

Yang Hang(杭阳), Wen-Zhi Wu(吴文志), Jin Yu(于进), Wan-Lin Guo(郭万林)
Chin. Phys. B . 2016, 25(2): 023102. **doi:** 10.1088/1674-1056/25/2/023102

Using the $Hg_xMg_{(1-x)}Te$ ternary compound as a room temperature photodetector: The electronic structure, charge transport, and response function of the energetic electromagnetic radiation

Ghasemi Hasan† and Mokhtari Ali

Department of Physics, Faculty of Sciences, Shahrekord University, P. O. Box 115, *Shahrekord, Iran*

(Received 8 November 2017; revised manuscript received 16 January 2018; published online 26 April 2018)

In the present work, firstly, a first-principles study of the structural, electronic, and electron transport properties of the $Hg_xMg_{(1-x)}Te$ (HMT) ternary compound is performed using the ABINIT package and the results are compared with $Cd_{0.9}Zn_{0.1}Te$ (CZT) as a current room-temperature photodetector. Next, the response functions of $Hg_{0.6}Mg_{0.4}Te$ and $Cd_{0.9}Zn_{0.1}Te$ under electromagnetic irradiation with 0.05 MeV, 0.2 MeV, 0.661 MeV and 1.33 MeV energies are simulated by using the MCNP code. According to these simulations, the $Hg_{0.6}Mg_{0.4}Te$ ternary compound is suggested as a good semiconductor photodetector for use at room temperature.

Keywords: band gap, charge-carrier transport, photodetector, density functional theory

PACS: 31.15.E, 31.15.es, 29.40.–n, 29.30.Kv **DOI:** 10.1088/1674-1056/27/5/053101

1. Introduction

Semiconductor photodetectors are used to detect electromagnetic radiation. The high resolution and efficiency of semiconductor photodetectors depend on a high atomic number (Z), a small band gap and, finally, a high product value of charge-carrier mobility and free electron–hole lifetime. On the other side, at room temperature (RT), an unwelcome dark current is produced by thermal noises and leakage currents in the photodetector. At RT, the dark current is negligible provided there is high electrical resistivity ($\geq 10^9$ Ω·cm) and a proper band gap (about 1.5 eV)[1,2]. Nowadays, the binary and ternary compounds of the II–VI groups are extensively used in spectroscopy, such as frozen $Hg_xCd_{(1-x)}Te$[3] and $Zn_xHg_{(1-x)}Te$ with $x < 0.5$[4] for IR spectroscopy and CdTe or $Cd_{0.9}Zn_{0.1}Te$ for energetic electromagnetic radiation (including the ultraviolet, x and gamma rays) spectroscopy at RT.

In order to achieve an appropriate option for RT detection comparable to $Cd_{0.9}Zn_{0.1}Te$, we propose the $Hg_{0.6}Mg_{0.4}Te$ ternary compound. In this research, we investigate this claim by using the computational approach. We study its band gap, electron mobility and response function to the energetic electromagnetic radiation, mechanical properties, and electrical resistivity.

The HgTe binary compound[5] is a semimetal with a narrow and negative band gap, huge spin–orbit coupling (SOC) interaction,[6] high atomic numbers of Hg and Te atoms, and high electron mobility.[7] On the other hand, natural magnesium telluride (MgTe) has a wurtezite structure, but thanks to new material synthesis methods such as molecular beam epitaxy (MBE) and metal-organic chemical vapor deposition (MOCVD), the production of the zinc blende (ZB) structure of MgTe (β-MgTe) is possible. Its band gap is wide and its charge mobility is low.[7] In the present work, we use the ZB phase of the MgTe compound and concentrate it with Hg atoms to simulate the HMT ternary alloy.

Previous research on the $Hg_xMg_{(1-x)}Te$ (HMT) ternary compound[8–10] involved density functional theory (DFT) simulations or experimental measurements of the structural and electronic properties of the binary and ternary compounds without charge transport consideration, and indicated that doping of the Hg atoms inside β-MgTe reduces the β-MgTe band gap. The mechanical properties of the II–VI compounds were studied in Refs. [11] and [12]. In the present work, in order to achieve a complete investigate of the feasibility of using the $Hg_xMg_{(1-x)}Te$ ternary compound as a good RT photodetector, we study as a first step the structural and electronic properties of the β-MgTe (shortened name, MgTe) and HMT including the band structure, band gap and effective masses of the electron and hole. In the next step, we simulate the optical properties of the HMT including the static dielectric constant, infinite dielectric constant and optical phonons energies. Then we calculate the charge-carrier mobility of the HMT. These calculations give the optimal Hg and Mg atom concentrations in the HMT. With these optimal values, we simulate the response function of the HMT under electromagnetic irradiation. We present the elastic stiffness tensor elements of this optimum compound, which are the major basis of the mechanical properties calculations. Finally, we report the electrical resistivity. We repeat the other DFT calculations[8,9] using generalized gradient approximation (GGA) pseudopotentials in the presence of SOC, in addition to the GW approximation correction.

†Corresponding author. E-mail: nifa2616@gmail.com

© 2018 Chinese Physical Society and IOP Publishing Ltd

The rest of the paper is organized as follows. Section 2 gives details of the computational methodology and some important parameters. The results and discussion concerning the band structure, electron mobility, response function, mechanical properties and electrical resistivity are given in Section 3. Finally, the concluding remarks of our work are summarized.

2. Computational details

In this work, firstly, the ABINIT[13] package is used to simulate the electronic and transport quantities of compounds and, next, the MCNP[14] package is used to simulate the energetic electromagnetic radiation interactions with matter.

ABINIT as an open source code, works within DFT, using pseudopotentials and a plane-wave basis set. In our DFT calculations,[15,16] the Trouiller–Martins,[17] Perdew–Burke–Ernzerhof,[18] and Hartwigsen–Goedecker–Hutter (HGH)[19] types of the exchange–correlation functional are used. The kinetic energy cut off for the wave functions expansion is optimized at about 30 Hartree. The lattice constants of the HgTe, MgTe and HMT compounds are theoretically estimated by the convergence threshold of total energy less than 0.0001 Hartree. A $4\times4\times4$ $\boldsymbol{k}$-points mesh is optimized by using the Monkhorst–Pack approach.

In the present work, according to the acceptable accuracy and speed of calculations, the alchemical mixing of pseudopotentials known as virtual-crystal approximation (VCA) method is used for ternary alloy semiconductor simulations instead of the supercell method. The VCA method is used to transform an ordered structure into a disordered structure within DFT approach calculations. In the VCA, the main idea is to introduce an element whose properties would reflect the properties of the two atoms simultaneously at a given proportion. This approach is simply a linear combination of two one-electron potentials describing pure crystals.

The relativistic norm-conserving pseudopotentials of the ion cores of Hg, Mg and Te can be written as[20]

$$V^{\text{ion}}_{\text{pseudo.}}(r)=\sum_{l}|l><[V^{\text{ion}}_{l}(r)+V^{\text{so}}_{l}(r)\,\boldsymbol{L}\cdot\boldsymbol{S}]<l|, \qquad (1)$$

where the average pseudopotential is

$$V^{\text{ion}}_{l}(r)=\left(\frac{1}{2l+1}\right)\left[(l+1)V^{\text{ion}}_{l+1/2}(r)+lV^{\text{ion}}_{l-1/2}(r)\right], \qquad (2)$$

and the spin–orbit coupling correction potential is

$$V^{\text{SOC}}_{l}(r)=\left(\frac{2}{2l+1}\right)\left[V^{\text{ion}}_{l+1/2}(r)-V^{\text{ion}}_{l-1/2}(r)\right]. \qquad (3)$$

Here $V^{\text{ion}}_{l+1/2}(r)$ and $V^{\text{ion}}_{l-1/2}(r)$ are the relativistic core pseudopotentials for spin-up and spin-down valence electrons, respectively. For the $Hg_xMg_{(1-x)}Te$ ternary compound under the VCA method, the pseudopotential at point $\boldsymbol{r}$ due to all ion cores is given by

$$V^{\text{VCA}}_{\text{pseudo.}}(\boldsymbol{r})=\sum_{i,j}[xV^{\text{Hg}}(\boldsymbol{r}-\boldsymbol{R}_i)+(1-x)V^{\text{Mg}}(\boldsymbol{r}-\boldsymbol{R}_i)+V^{\text{Te}}(\boldsymbol{r}-\boldsymbol{R}_j)]. \qquad (4)$$

It has been shown for different ternary compounds that the obtained results by super-cell and VCA methods have acceptable agreements.[20–22]

The MCNP is a general-purpose Monte Carlo N-particle code that can be used for neutron, photon, electron or coupled neutron/photon/electron transport using cross-section data. Given some inputs, the MCNP returns the dose, flux, response function, etc. In our calculations, we use ENDF/B-VI interaction cross-sections, a crystal cylindrical geometry with 3.81 cm radius and 7.62 cm height and an electromagnetic radiation point source with 10^9 incident photon number, 0.05 MeV, 0.2 MeV, 0.661 MeV and 1.33 MeV energies, and 0.01 cm distance to the detector.

3. Results and discussion

3.1. Electronic structure of HMT

The GGA approximation and HGH type pseudopotentials in the presence of SOC interaction are used to obtain the physical quantities of the HgTe and MgTe compounds, which show a good agreement with the experimental values. The obtained results are given in the following sections. This approach is used to calculate the effective mass, static dielectric constant and optical phonon energies; and the more precise approach, the GW approximation, is used to calculate the energy band gap.[13] The orbital structure of the $_{80}$Hg atom is $[_{54}Xe]4f^{14}5d^{10}6s^2$. Since the d orbital is full, the choice of the core and valence electrons is effective to calculate the band structure. To simulate such atoms, the number of valence electrons, z^{ion}, is selected as 2 or 12.

The band structures of the MgTe compound are calculated by both GGA and GW approximation approaches and presented in Figs. 1(a) and 1(b). The calculated energy band gaps by the GW approximation approach at the L, Γ and X points are 3.98 eV, 3.3 eV and 3.38 eV, respectively. The experimental energy band gap of MgTe is 3.4 eV[7] in good agreement with the calculated value. To investigate the effect of the SOC interaction on the band structure of HgTe, the band structures of this compound in the presence of SOC (Fig. 1(c)) and without SOC (Fig. 1(d)) with $z^{\text{ion}}=2$ are obtained. Our obtained result in Fig. 1(d) is in good agreement with that in the other work.[5] Due to the huge spin–orbit interaction in HgTe, the degeneracy of the heavy-hole and light-hole bands is removed at $k=0$, and inversion of the valence and conduction bands occurs.[5]

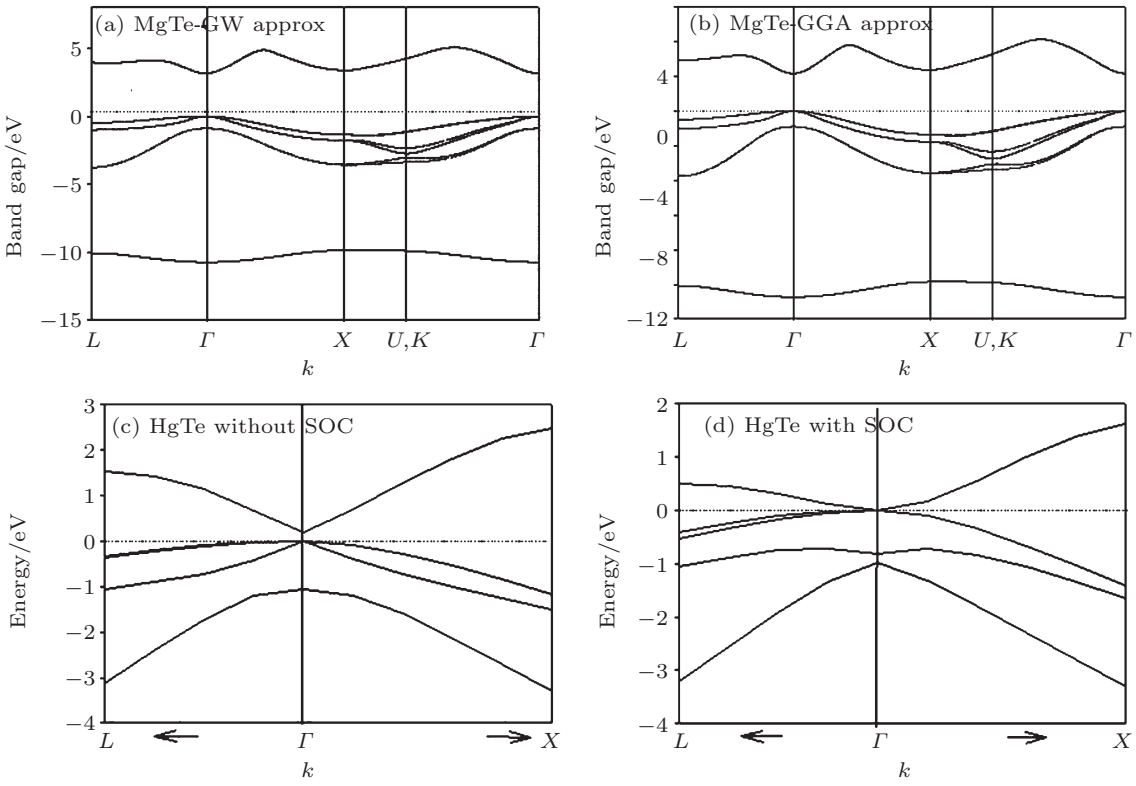


Fig. 1. The band structure of the MgTe (a) by the GW approximation in the presence of SOC interaction, (b) by the GGA and HGH-type pseudopotentials in the presence of SOC interaction, and the band structure of the HgTe in the vicinity of the Γ point (c) without and (d) with SOC. The Fermi energy is set to zero.

Figure 2 shows the calculated band gap of the HMT versus x, based on two approaches: GGA in the presence of SOC and GW in the presence of SOC. The obtained results based on the GW approach are in good agreement with the experimental one of the MgTe compound (ZB phase).

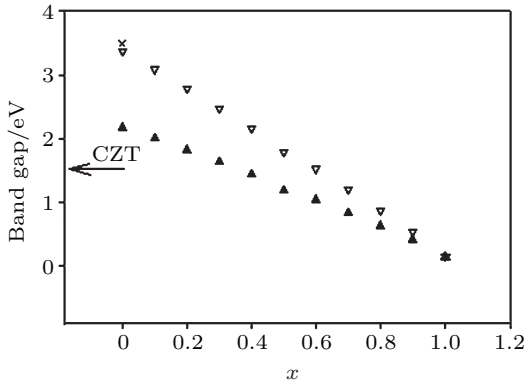


Fig. 2. The calculated band gap of the HMT as a function of x by GGA (solid triangle) and the GW approach (hollow triangle) in the presence of SOC compared to the MgTe (cross)[7] and CZT[2] experimental values.

In an electrical circuit, unwelcome thermal noises on the surface of a semiconductor with band gap less than 1.5 eV are seriously produced. On the other hand, the number of photo-produced electron–hole pairs inside a semiconductor with band gap greater than 2 eV is few. Thus the optimum energy band gap for the RT photodetector is about 1.5 eV. According to Fig. 2, the energy band gap of the HMT compound varies in the range of 0 to 3.4 eV and at $x \cong 0.6$, the energy gap requirement of a good RT photodetector is satisfied.

The underestimating of band gap in DFT using traditional approximations for the exchange–correlation term (such as GGA) is related to the fact that such approaches cannot simultaneously obtain the exchange–correlation energy and its charge derivative accurately.[23] Using the Green function (GW) approach and considering the self-energy contributions, we can overcome this deficiency of the DFT. The improvement is clearly shown in Fig. 2. For MgTe, the underestimation of the band gap energy is about 3.4%. The band gaps are direct as a welcome object for photo-detection devices.

3.2. Electrical transport properties

According to the obtained result of the previous section, the $Hg_xMg_{(1-x)}Te$ ternary compound with $x \cong 0.6$ satisfies the requirement for an RT photodetector energy gap. However, calculations of the charge-carrier transport properties are needed to ensure the feasibility of using this compound as an efficient RT photodetector.

The most important electronic scattering processes relevant to the charge-carrier mobility in semiconductors include[24–26] deformation potential scattering, piezoelectric phonon scattering, polar optical phonon scattering, ionized impurity scattering, alloy scattering and other electron scattering types.

The total charge-carrier mobility depends on the sec-

ondary mobility by the Matthiessen rule[25,26]

$$\frac{1}{\mu} = \frac{1}{\mu_1} + \frac{1}{\mu_2} + \cdots . \tag{5}$$

At RT, the mobility is essentially controlled by the polar optical phonons and the total mobility is approximately equal to the mobility caused by polar optical phonon scattering[25,26]

$$\begin{aligned} \mu_{\text{total}} &= \mu_{\text{polar optical phonons}} \\ &= \frac{3\left(2\pi\hbar\omega_{\text{LO}}\right)^{1/2}}{4m^{1/2}E_0 n\left(\omega_{\text{LO}}\right)x_0^{3/2}\,\mathrm{e}^{x_0/2}K_1\left(x_0/2\right)}, \end{aligned} \tag{6}$$

$$n\left(\omega_{\text{LO}}\right) = \frac{1}{\left[\mathrm{e}^{x_0}-1\right]},\quad x_0 = \frac{\hbar\omega_{\text{LO}}}{K_{\text{B}}T},$$

$$E_0 = \frac{me\hbar\omega_{\text{LO}}\left(1/\varepsilon^{\infty}-1/\varepsilon^{0}\right)}{4\pi\hbar^2}, \tag{7}$$

where $K_1(t)$ is the Bessel function

$$K_1(t) = t\int_1^{\infty}\left(z^2-1\right)^{1/2}\mathrm{e}^{-tz}\mathrm{d}z. \tag{8}$$

Here k_{B}, T, $\hbar$, m, ω_{LO}), $n(\omega_{\text{LO}})$, ε^0 and ε^{∞} are the Boltzmann constant, Kelvin temperature, reduced Planck constant, free-charge-carrier mass, longitudinal optical phonon frequency, Bose–Einstein distribution function, static dielectric constant and high frequency dielectric constant, respectively.

The static dielectric constant and high frequency dielectric constant are related to the transverse and longitudinal modes of the optical phonons by the Lyddane–Sachs–Teller equation[25,26]

$$\frac{\varepsilon^0}{\varepsilon^{\infty}} = \left(\frac{\omega_{\text{LO}}}{\omega_{\text{TO}}}\right)^2. \tag{9}$$

For estimating the electron mobility, we calculate a) the electron effective mass: this quantity is obtained as the second derivative of the energy respect to the $\boldsymbol{k}$ vector at the Γ point of the band structure $m^* = \hbar^2(\mathrm{d}^2E/\mathrm{d}k^2)^{-1}$, b) the longitudinal and transverse optical phonon energies: these quantities are obtained by the frequencies at the Γ point of the phonon dispersion curve as an output of the ABINIT code, c) the static dielectric constant: this quantity is obtained by the polarization curve with respect to the applied external electrical field as an output of the ABINIT code, and d) the high frequency dielectric constant: this quantity is obtained by Eq. (9) using the optical phonon frequencies. For HMT, figure 3 shows the electron effective mass, the static dielectric constant, and the longitudinal and the transverse phonon energies, as compared to the experimental values.[7]

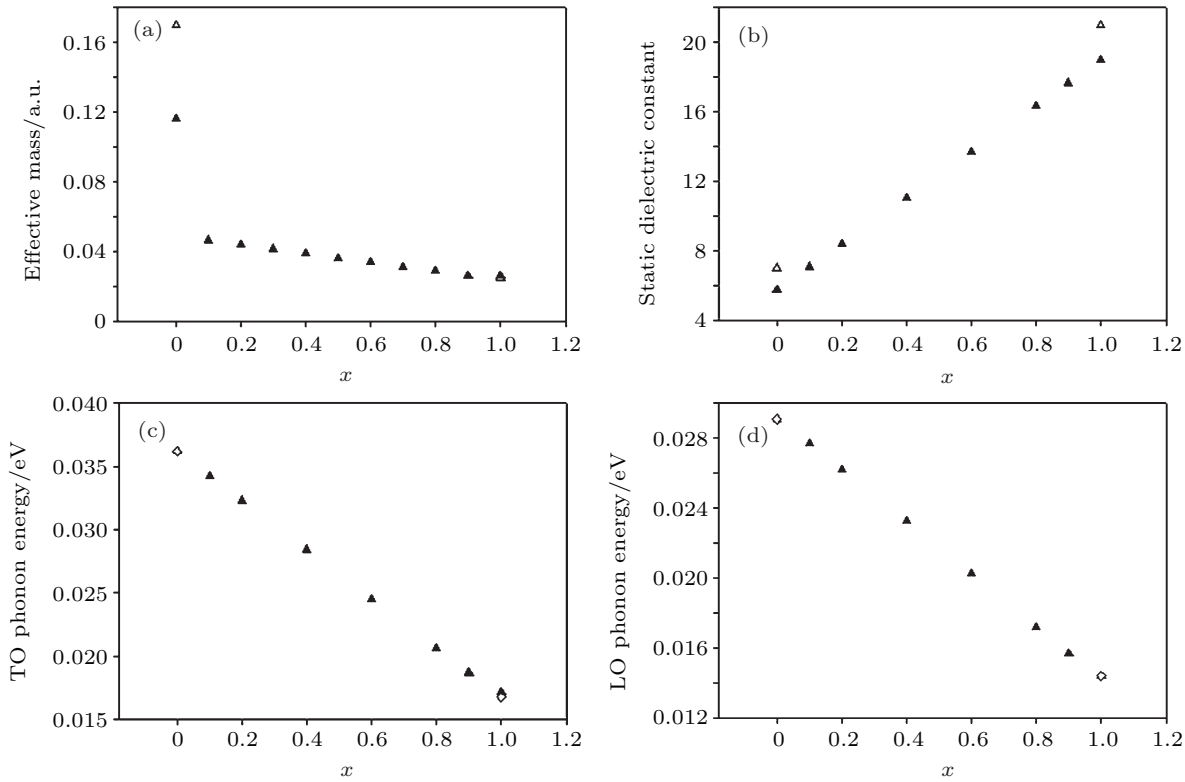


Fig. 3. (a) Electron effective masses, (b) the static dielectric constant, (c) transverse and (d) longitudinal optical phonons energies of the HMT as a function of x (solids), compared to the experimental values[7] (hollows).

According to Fig. 3(a), it is seen that the effective mass of the HMT decreases with increasing substitution of Hg for Mg atoms, because of the tiny effective mass of the HgTe as the second-order derivative of valence and conductance bands at $k = 0$.[5] This is the result of the SOC effects on the valence and conductance bands of HgTe in the vicinity of the Γ point. The underestimations of this parameter for MgTe and HgTe compounds are about 29% and less than 1%, respectively. As

we can see in Fig. 3(b), the static dielectric constant of the HMT increases with increasing x because of the great polarization vector and static dielectric constant of HgTe.[7] The underestimations of this parameter for MgTe and HgTe compounds are about 18% and 22%, respectively. In Figs. 3(c) and 3(d), it is seen that the optical phonon energies of the HMT decrease with increasing x because of the larger Hg core mass than that of Mg atoms. The optical phonon energy is inversely proportional to the core mass. The underestimation of these parameters for both MgTe and HgTe compounds is less than 1%. The calculated physical quantities of the MgTe and HgTe compounds are presented in Table 1. The calculated values are in good agreement with those in other work.[7]

Table 1. Simulated and experimental charge-transport quantities of MgTe and HgTe compounds.

	MgTe		HgTe	
	our work	others[7]	our work	others[7]
Electron effective mass[a]/a.u.	0.12	0.17	0.03	0.031
Heavy hole effective mass/a.u.	0.5	0.46	0.26	0.28
Light hole effective mass/a.u.	0.34	0.24	−0.03	−0.029
Longitudinal optical phonon energy/cm^{-1}	292	292	138	135
Transverse optical phonon energy/cm^{-1}	230	235	115	116
Static dielectric constant	5.74	7	19	21

[a] $\Gamma \rightarrow X$.

Figure 4 shows the electron mobility of the HMT. For MgTe and HgTe compounds, our underestimations are less than 1% and 24%, respectively. Since the effective mass of a hole in the semiconductor is manifold of the effective mass of an electron, the total mobility is equal to the electron mobility. According to Fig. 4, the electron mobility of the HMT increases with increasing substitution of Hg atoms rather than Mg atoms because of the reducing of the effective mass. The charge mobility is strongly proportional to the charge effective mass. This figure shows that, from an electron mobility point of view, $Hg_xMg_{(1-x)}Te$ with $x \cong 0.6$ competes well with the $Cd_{0.9}Zn_{0.1}Te$ ternary compound.[1]

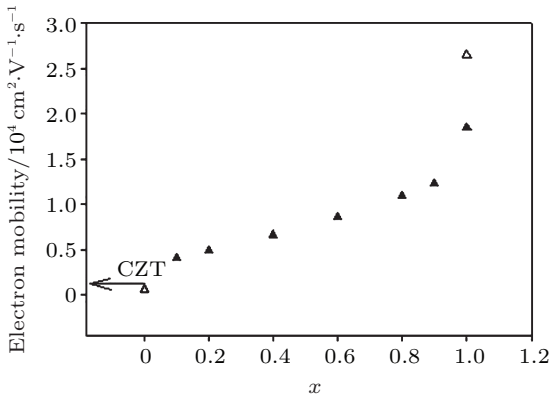


Fig. 4. Calculated electron mobility of the HMT at $T = 300$ K compared to the HgTe, MgTe,[7] and CZT[2] experimental values (hollow). The total mobility is equal to the electron mobility because of the heavy effective mass of a hole relative to that of an electron.

Based on the obtained results in this section and the previous section, the optimum x value of 0.6 is suggested. In the next section, the response functions of the $Hg_{0.6}Mg_{0.4}Te$ and $Cd_{0.9}Zn_{0.1}Te$ compounds to the energetic electromagnetic radiations are calculated by the MCNP package and compared.

3.3. Response function

The basis of radiation detection by semiconductor crystals is the production of the free electrons and holes under irradiation of the crystal. The output of the irradiated crystal is an electrical signal described by the response function or pulse height distribution and is collected by electronic systems. The response functions can be calculated by one of three different ways: experimental, Monte Carlo or semi-empirical methods. One of the abilities of the MCNP code is the response function generation by the Monte Carlo method.[22] The photon energy regime in MCNP is from 1 keV to 1 GeV. Since the electromagnetic radiation in the x and gamma regions is used abundantly in industrial, medicine and research fields, we calculate the response function to the energetic electromagnetic radiations for the $Hg_{0.6}Mg_{0.4}Te$ and $Cd_{0.9}Zn_{0.1}Te$ by MCNP in these regions with 0.05 MeV, 0.2 MeV, 0.661 MeV and 1.33 MeV radiation energies. The presented response functions in Fig. 5 show that the $Hg_{0.6}Mg_{0.4}Te$ compound is comparable to the $Cd_{0.9}Zn_{0.1}Te$ compound in all energy ranges of the incident radiation. According to Fig. 5, the resolution and efficiency of the $Hg_{0.6}Mg_{0.4}Te$ compound are comparable to those of the $Cd_{0.9}Zn_{0.1}Te$ compound. This is because of the high atomic number of the Hg atoms.

3.4. Mechanical properties

When doping an impurity inside a semiconductor, it is necessary to investigate its mechanical properties.[1] When there is interaction between a native defect and an impurity or between the lattice and an impurity, lattice relaxation occurs locally to minimize the energy. An impurity in a lattice that causes significant lattice relaxation is called the DX-center.

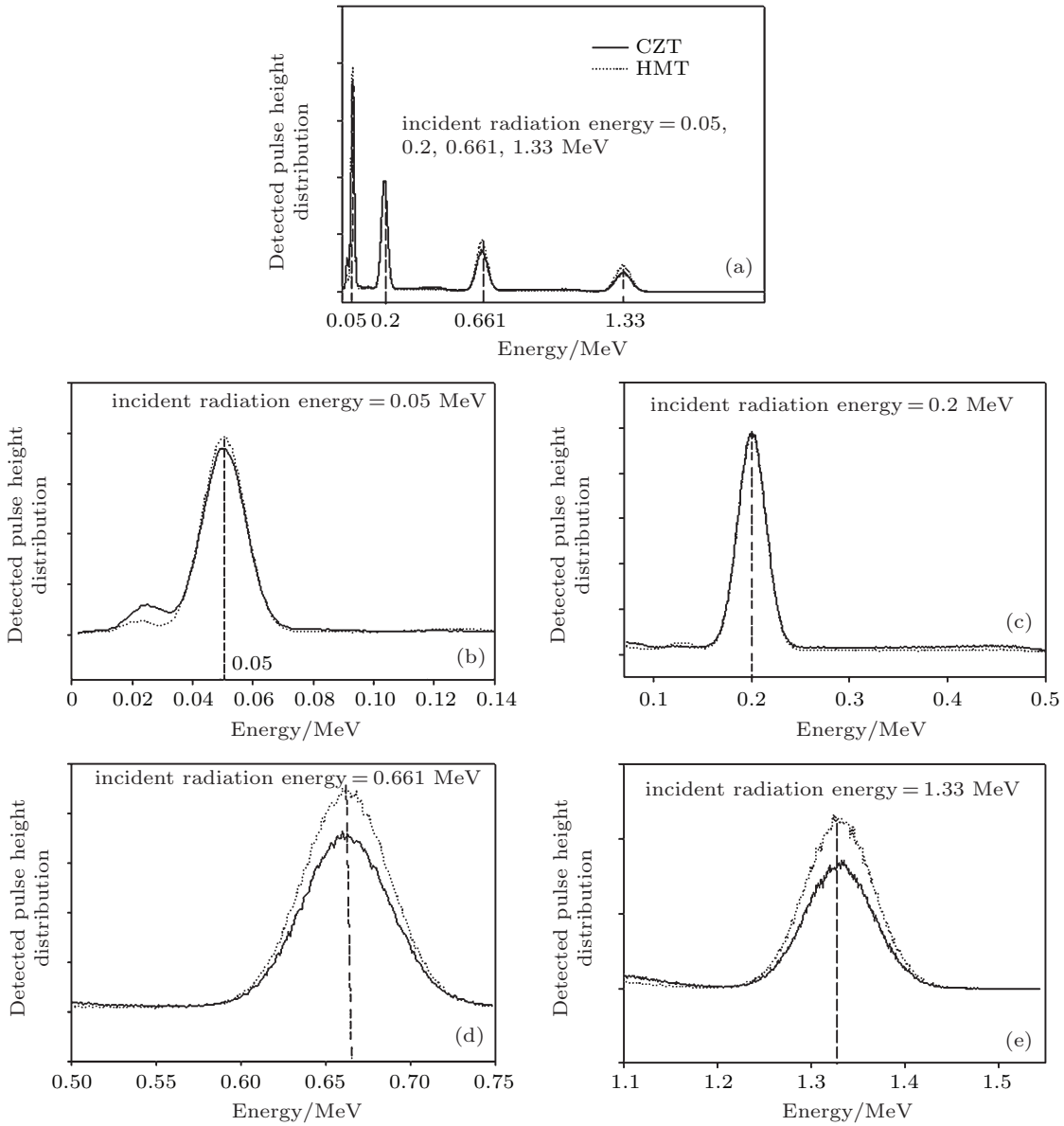


Fig. 5. (a) Response functions of the $Hg_{0.6}Mg_{0.4}Te$ (dotted line) and $Cd_{0.9}Zn_{0.1}Te$ (solid line) compounds for different energetic electromagnetic radiations and separated spectra with energies of (b) 0.05 MeV, (c) 0.2 MeV, (d) 0.661 MeV and (e) 1.33 MeV.

Using the calculated quantities in the previous sections, such as m, ε^0 and ε^∞, we are able to obtain the mechanical properties of the $Hg_{0.6}Mg_{0.4}Te$ ternary compound. The elements of the elastic stiffness tensor are the principal quantities.[7,11,12]

The elements of this tensor are used to calculate the thermal and mechanical quantities of the materials, such as the Debye temperature, elastic stress tensor, elastic strain tensor, Young's modules, Poisson's ratio, bulk modules, shear modulus, isotropy factor, linear compressibility, Cauchy ratio, Born ratio, micro-hardness and sound velocity.[27] We use the following relations to calculate the c_{11}, c_{12} and c_{44} elements:[11]

$$c_{11} = \frac{\sqrt{3}\hbar^2 \left(1-\alpha_p^2\right)^{1/2} \left(4.37\left(5+\lambda\right)\left(1-\alpha_p^2\right)-0.6075\right)}{4d^5 m}, \tag{10}$$

$$c_{12} = \frac{\sqrt{3}\hbar^2 \left(1-\alpha_p^2\right)^{1/2} \left(4.37\left(3-\lambda\right)\left(1-\alpha_p^2\right)-0.6075\right)}{4d^5 m}, \tag{11}$$

$$c_{44} = \frac{3(c_{11}+2c_{12})(c_{11}-c_{12})}{7c_{11}+2c_{12}}, \tag{12}$$

where m, d and α_p are the electron effective mass, nearest-neighbor distance and polarity, respectively, and

$$\lambda = 0.738, \quad \frac{\varepsilon^0-1}{\varepsilon^\infty-1} - 1 = \frac{\alpha_p^2\left(1+2\left(1-\alpha_p^2\right)\right)}{2\left(1-\alpha_p^2\right)^2}. \tag{13}$$

According to the results of the previous sections, we present the elastic stiffness tensor elements of the HgTe, MgTe and $Hg_{0.6}Mg_{0.4}Te$ compounds. Table 2 presents these elements compared to other works.

As we can see, the c_{11}, c_{12} and c_{44} elements of the HgTe and MgTe binaries and $Hg_{0.6}Mg_{0.4}Te$ ternary compounds are approximately equal,[7] which is a favorable condition for the formation of DX-centers inside the $Hg_{0.6}Mg_{0.4}Te$ ternary compound.[1]

Table 2. The elements of the elastic stiffness tensor.

Material	$c_{11}/10^{10}$ Pa		$c_{12}/10^{10}$ Pa		$c_{44}/10^{10}$ Pa	
	our work	others work[7]	our work	others work[7]	our work	others work[7]
HgTe	5.29	5.32	3.08	3.68	2.62	2.08
MgTe	4.878	5.28	3.479	3.66	1.60	1.93
$Hg_{0.6}Mg_{0.4}Te$	5.04		3.32		2.01	

3.5. Electrical resistivity

For RT photodetectors, high resistivity is necessary (threshold value $> 10^7$ Ω·cm, excellent value $> 10^9$ Ω·cm) to reduce leakage currents and unwelcome noises.[1,2] The electrical resistivity is given by[28]

$$R = 1/\sigma = 1/(ne\mu_e + pe\mu_h), \tag{14}$$

where R, σ, n, p, μ_e and μ_h are the electrical resistivity, electrical conductivity, the density of thermal-produced free electrons and holes, and electron and hole mobilities, respectively.

The density of the thermal-produced free electron–hole pairs in the unit volume of an intrinsic semiconductor crystal is given by[28]

$$n = p, \;\; np = 4\left(\frac{k_B T}{2\pi\hbar^2}\right)^3 (m_e m_h)^{3/2} e^{-E_g/k_B T}, \tag{15}$$

where m_e, m_h and E_g are the free electron and hole effective masses and the band gap, respectively. In Table 3, the obtained electrical resistivity of the $Hg_{0.6}Mg_{0.4}Te$ compared to the two current RT photodetectors CZT[2] and GaAs[2] is given. As we can see the $Hg_{0.6}Mg_{0.4}Te$ electrical resistivity is not excellent, but acceptable and comparable to that of the GaAs compound.

Table 3. The obtained electrical resistivity of the $Hg_{0.6}Mg_{0.4}Te$ compared to CZT[2] and GaAs.[2,7]

Material	m_e/a.u.	m_{lh}/a.u.	m_{hh}/a.u.	E_g/eV	μ_e/(cm^2/V·s)	μ_h/(cm^2/V·s)	R/Ω·cm
CZT	0.09[a]	0.16[a]	0.5[a]	1.59[a]	1000[a]	120[a]	3×10^{10}[a]
GaAs	0.07[b]	0.09[b]	0.33[b]	1.43[b]	8000[a]	400[a]	10^7[a]
$Hg_{0.6}Mg_{0.4}Te$	0.08	0.12	0.35	1.45	15000	200	3×10^7

[a] Ref. [2], [b] Ref. [7].

4. Conclusion

In the present work, the electronic structure and transport properties of the $Hg_xMg_{(1-x)}Te$ ternary compound, as a combination of MgTe and HgTe binary compounds, are theoretically studied. This study is based on the simulation of the HMT by the ABINIT package and the results indicate that addition about 60% Hg to MgTe satisfies the requirements of a good RT photodetector. These simulations, including the response function simulation by the MCNP package, introduce $Hg_{0.6}Mg_{0.4}Te$ as an ideal RT photodetector for x and gamma rays spectroscopy, comparable to the $Cd_{0.9}Zn_{0.1}Te$ compound.

Acknowledgment

This work was carried out in the Simulation Laboratory of the Physics Group with the support of Shahrekord University under project number 230689.

References

[1] Schlesingera T E, Toneyb J E, Yoonc H, Leed E Y, Brunettd B A, Franksd L and Jamesd R B 2001 *Mater. Sci. Eng.* **32** 103
[2] Owens A and Peacock A 2004 *Nucl. Instrum. Methods Phys. Res. Sect. A* **531** 18
[3] Kim J J 2012 *Characterization of HgCdTe and Related Materials and Substrates for Third Generation Infrared Detectors* (PhD Thesis: Arizona State University) p. 1
[4] Rogalski A 1989 *Quantum Electronics* **13** 299
[5] Svane A, Christensen N E, Cardona M, Chantis A N, Schilfgaarde M and Kotani T 2011 *Phy. Rev. B* **84** 205205
[6] Winkler R 2003 *Spin–Orbit Coupling Effects in Two-Dimensional Electron and Hole Systems* (Heidelberg: Springer) p. 61
[7] Aldachi S 2009 *Properties of Group – IV III-V and II-VI Semiconductors* (New York: John Wiley & Sons)
[8] Gokoglu G, Durandurada Mand Gulseren O *Comput. Mater. Sci.* **4** 7593
[9] Imad K, Fazie S, Iftikhar A and Zahid A 2015 *J. Phys. Chem. Solids* **83** 75
[10] Paesler K, Kiinig B, Truchsess M, Pfeuffer-Jeschke A, Oehling S, Becker C R and Batke E 1998 *J. Cryst. Growth* **184/185** 1209
[11] Mnasri S, Abdi-Ben Nasrallah S, Sfina N, Bouarissa N and Said M 2009 *Semicond. Sci. Technol* **24** 095008
[12] Shi C, Tu Q, Fan H and Li S 2016 *J. Micromech. Mol. Phys.* **1** 1650005
[13] Gonze X, Amadon B, Anglade P M, Beuken J M, Bottin F, Boulanger P, Bruneval F, Caliste D, Caracas R, Côté M, Deutsch T, Genovese L, Ghose Ph, Giantomassi M, Goedecker S, Hamann D R, Hermet P, Jollet F, Jomard G, Leroux S, Mancini M, Mazevet S, Oliveira M J T, Onida G, Pouillon Y, Range T, Rignanese G M, Sangalli D, Shaltaf R, Torrent M, Verstraete M J, Zerah G and Zwanziger J W 2009 *Comput. Phys. Commun* **180** 2582
[14] https://mcnp.lanl.gov/
[15] Hohenberg P and Kohn W 1964 *Phys. Rev. B* **136** 864
[16] Kohn W and Sham L J 1965 *Phys. Rev.* **140** A1133
[17] Troullier W and Martins J L 1991 *Phys. Rev. B* **43** 1993
[18] Perdew J, Burke K and Ernzerho M 1996 *Phys. Rev. Lett.* **77** 3865
[19] Hartwigsen C, Goedeckerand S and Hutter J 1998 *Phys. Rev. B* **58** 3641
[20] Poon H C, Feng Z C, Feng Y P and Li M F J 1995 *Phys. Condens. Matter* **7** 2783
[21] Bechiri A, Benmakhlouf F and Bouarissa N 2009 *Phys. Procedia* **2** 803
[22] Dargam T G, Capaz R B and Koiller B 1997 *Braz. J. Phys.* **27** 4
[23] Mokhtari A 2007 *J. Phys.: Condens. Matter* **19** 436213
[24] Tiwari S 1992 *Compound Semiconductor Device Physics* (New York: Academic Press) p. 7
[25] Jena D 2004 *Charge Transport in Semiconductors EE 698D Advanced Semiconductor Physics* (University of Notre Dame)
[26] Jacoboni C 2010 *Theory of Electron Transport a Pathway from Elementary Physics to Nonequilibrium Green Functions* (New York: Springer) p. 127
[27] Feng J, Xiao B, Chen J, Dua Y, Yua J and Zhou R 2011 *Mater. Des.* **32** 3231
[28] Kittel C 2005 *Introduction to Solid State Physics* (New York: John Willey & Sons) p. 185